THE JOURNAL OF BIOLOGICAL CHEMISTRY
Vol. 273, No. 38, Issue of September 18, pp. 24912–24920, 1998

Printed in U.S.A.

Mutations in and Monoclonal Antibody Binding to Evolutionary Hypervariable Region of *Escherichia coli* RNA Polymerase β′ Subunit Inhibit Transcript Cleavage and Transcript Elongation*

(Received for publication, March 5, 1998, and in revised form, July 16, 1998)

Natalya Zakharova‡, Irina Bass§, Elena Arsenieva§, Vadim Nikiforov§, and Konstantin Severinov‡¶‖

From the ‡Waksman Institute, Piscataway, New Jersey 08854, the ¶Department of Genetics, Rutgers, The State University of New Jersey, Piscataway, New Jersey 08854, and the §Institute of Molecular Genetics, Russian Academy of Sciences, Moscow 123182, Russia

A 190 amino acid-long region centered around position 1050 of the 1407-amino acid-long β′ subunit of *Escherichia coli* RNA polymerase (RNAP) is absent from homologues in eukaryotes, archaea and many bacteria. In chloroplasts, the corresponding region can be more than 900 amino acids long. The role of this hypervariable region was studied by deletion mutagenesis of the cloned *E. coli rpoC*, encoding β′. Long deletions mimicking β′ from Gram-positive bacteria failed to assemble into RNAP. Mutants with short, 40–60-amino acid-long deletions spanning β′ residues 941–1130 assembled into active RNAP *in vitro*. These mutant enzymes were defective in the transcript cleavage reaction and had dramatically reduced transcription elongation rates at subsaturating substrate concentrations due to prolonged pausing at sites of transcriptional arrest. Binding of a monoclonal antibody, Pyn1, to the hypervariable region inhibited transcription elongation and intrinsic transcript cleavage and, to a lesser degree, GreB-induced transcript cleavage, but did not interfere with GreB binding to RNAP. We propose that mutations in and antibody binding to the hypervariable, functionally dispensable region of β′ inhibit transcript cleavage and elongation by distorting the flanking conserved segment G in the active center.

DNA-dependent RNA polymerases from eubacteria share a common subunit composition (1). The core RNAP[1] enzyme (subunit composition $\alpha_2\beta\beta'$) is catalytically proficient but is unable to initiate transcription on promoters. Binding of a σ subunit converts the core enzyme into a holoenzyme, which can recognize a specific set of promoters (2). The β and β′ subunits together constitute more than 80% of the core RNAP mass and jointly form the catalytic center of the enzyme (3, 4). RNAPs from eukaryotes and archaea have subunits that are homologous to β and β′ of eubacterial enzymes (5–7). The evolutionary conservation within the β/β′ lineages is limited to relatively short segments of primary sequence; each subunit has 8–10 highly conserved segments. The amino- to carboxyl-terminal order of the conserved segments is invariant.

The spacing between the conserved segments can vary even when subunits from closely related species are compared, due to an accumulation of insertions and deletions. There are several reasons why studies of such evolutionarily variable regions can shed light on RNAP structure and function. First, these regions may form docking sites for species-specific regulators of transcription (8, 9). Second, variable regions are likely to be surface-exposed and can therefore be used for affinity tagging of RNAP and transcription complexes (10). Third, variable regions often tolerate splits, allowing preparation of functional RNAP with relatively short β and/or β′ subunit fragments, dramatically facilitating mapping of protein-protein and protein-nucleic acid contacts during transcription (11, 12).

The focus of this report is an evolutionary hypervariable region in the C-terminal portion of *Escherichia coli* β′ (amino acids 1141–1131). This region is highly variable in proteobacteria and is absent from homologs from most other bacteria, archaea, and eukaryotes. Despite this apparent redundancy, numerous point mutations that altered the termination and elongation properties of *E. coli* RNAP were localized in the hypervariable region (25, 37, 38). In addition, mutations in the largest (β′-like) subunit of yeast RNAP II that occurred very close to the hypervariable region dramatically decreased interaction of the enzyme with transcript cleavage factor TFIIS (33). Here, we probed the role of the hypervariable region and adjacent segments of *E. coli* β′ by deletion mutagenesis of the cloned *rpoC* gene. Mutant RNAPs were assembled *in vitro*, and their elongation and termination properties, as well as their abilities to interact with the TFIIS analog GreB, were determined. A long deletion that completely removed the hypervariable region blocked enzyme assembly *in vivo* and *in vitro*. Short (40–60 amino acid) deletions, which together span the entire hypervariable region, did not prevent RNAP assembly and basic transcription function *in vitro*; however, the mutant enzymes had a dramatic defect in transcript elongation at low substrate concentrations. At high substrate concentrations, the mutants elongated and terminated transcription normally. The mutant enzymes were also defective in GreB-induced transcript cleavage, but the nature of the defect was complex, because both the ability to interact with GreB and the ability to support intrinsic transcript cleavage by the RNAP catalytic center were altered by mutations. A binding epitope for an inhibitory mAb, Pyn1, was mapped in the hypervariable region. Binding of Pyn1 to RNAP efficiently inhibited both the RNA synthesis and transcript cleavage reactions.

* This work was supported by The Borroughs Wellcome Fund for Biomedical Research Career Award, by the start-up funds from Rutgers University (to K. S.), and by Research Grants 96-04-49019 and 96-1598076 from the Russian Foundation for Basic Research and INTAS-RFBR Grant 9501150 (to V. N.). The costs of publication of this article were defrayed in part by the payment of page charges. This article must therefore be hereby marked "*advertisement*" in accordance with 18 U.S.C. Section 1734 solely to indicate this fact.

‖ To whom correspondence should be addressed. Tel.: 732-445-6095; Fax: 732-445-5735; E-mail: severik@waksman.rutgers.edu.

[1] The abbreviations used are: RNAP, RNA polymerase; EC^n, elongation complex stalled at position +n of the template, mAb, monoclonal antibody; PAGE, polyacrylamide gel electrophoresis; UTP, uridine triphosphate; WT, wild-type; HMPK, heart muscle protein kinase.

Our data thus demonstrate that the evolutionary hypervariable region of β′, which is completely absent from homologues from eukaryotes, archaea, and many eubacteria, is unexpectedly important for *E. coli* RNAP assembly and is involved in transcript elongation and cleavage. Because this region is missing from β′ homologues from most organisms, however, this involvement is probably indirect.

MATERIALS AND METHODS

Deletion Mutagenesis of the Cloned rpoC Gene—The pUC19-based pMKa201*S793F rpoC* expression plasmid was used to generate deletions in the *rpoC* gene. The plasmid is a derivative of pMKA201 (13) and carries a transdominant streptolydigin-resistance mutation, changing β′ Ser^{793} to Phe (14). To generate nested *Bal*31 deletions in pMKa201*S793F*, a unique *Bam*HI linker was inserted in the *Eco*RI site at codon 987 of the structural gene. pMKa201*S793F* was underdigested with *Eco*RI (cut twice at codons 175 and 987 of the structural gene and once in the vector), and ligated to the *Eco*RI fragment from phage mp17Km carrying the kanamycin resistance gene (11). Kanamycin-resistant transformants were screened for the appearance of inducible truncated fragments of the β′ polypeptide using SDS-PAGE. Recombinant plasmids containing kanamycin cassette inserted at *rpoC* position 987 was treated with *Bam*HI to remove the cassette and recircularized. The resultant plasmid pIBΩ*987* overproduced β′ with 6 amino acids (IPRIRG) inserted between amino acids 987 and 988.

To generate deletions, pIBΩ*987* was linearized with *Bam*HI, treated with *Bal*31 for various times, and recircularized. After transformation in *E. coli* XL1-Blue cells, transformants were screened for the appearance of inducible β′ polypeptides with increased mobility on SDS-gels.

pIBΔ*(1145–1198)* was constructed by treating pMKa201*S793F* with *Asu*I (cut twice at codons 1145 and 1198 of the structural gene) and religating. pIBΔ*(1091–1130)* was constructed from a plasmid expressing the C-terminal portion of *rpoC* ($β'^{877–1407}$, Ref. 12), containing two in-frame *Kpn*I recognition sites corresponding to *rpoC* codons 1091 and 1130. The *rpoC* fragment containing the deletion was then recloned back into pMKa201*S793F*.

Plasmids expressing Δ(877–948), Δ(941–1130), Δ(1042–1091), and Δ(1131–1155)S were constructed by annealing a pair of corresponding "outward" primers, followed by polymerase chain reaction amplification of the whole pMKa201*S793F* plasmid (30 cycles of 1 min at 94 °C, 1 min at 56 °C, and 8 min at 72 °C). Each primer used in the amplification reaction contained an in-frame *Bam*HI site. The amplified plasmid was treated with *Bam*HI, recircularized, and transformed in XL1-Blue cells. Transformants were screened for the appearance of inducible β′ polypeptides with increased mobility on SDS-gels, and deletions were confirmed by DNA sequencing. To minimize polymerase chain reaction-related errors, deletions were recloned as *Sal*I-*Sac*II (cut at *rpoC* codons 877 and 1321, respectively) fragments back into appropriately treated parental pMKa201*S793F*.

All of the overexpressed β′ subunit variants were found in inclusion bodies when induced with 1 mM IPTG at 37 °C.

Antibodies—mAbs Pyn1 and Pyn4 were described previously (15). mAbs were precipitated from ascites fluid by addition of $(NH_4)_2SO_4$ to 50% saturation. Before use, aliquots of precipitated protein were dialyzed into transcription buffer. Some mAb preparations contained an RNase activity. Hence, transcription reactions were supplemented with 0.5 mg of tRNA to prevent the degradation of RNA in transcription complexes. The working concentration of mAb was determined by combining a fixed amount of RNAP with increasing amounts of mAb, followed by separation of protein complexes on native 4–15% Phast gels (Amersham Pharmacia Biotech). The amount of mAb used in transcription reactions was twice the amount needed to shift completely the band of RNAP on a native gel.

RNAP Reconstitution—RNAP was reconstituted according to the published procedure (16). The molar ratio of α, β, and mutant β′ in the reconstitution reactions was 1:4:8. After reconstitution and thermoactivation in the presence of $σ^{70}$, RNAP preparations were either used directly or further purified by FPLC/gel-filtration on a Superose-6 and Mono Q columns (Amersham Pharmacia Biotech) as described (17), concentrated by filtration through a C-100 concentrator (Amicon) to ~1 mg/ml, and stored in 50% glycerol storage buffer at −20 °C.

Affinity Cross-linking—The synthesis of photoactive 4-azidotetrafluorobenzylamino-pApUpC derivative will be described elsewhere (18).[2] A standard 20-μl cross-linking reaction contained 0.5–1 μg of RNAP holoenzyme immobilized on ~5 μl of Ni^{2+}-NTA agarose (Qiagen), 0.5 μg of the 324-base pair DNA fragment containing T7 A1 promoter (template 1 of Ref. 18), and 10 μM ApUpC in standard transcription buffer containing 40 mM KCl, 40 mM Tris-HCl, pH 7.9, 10 mM $MgCl_2$. Reactions were incubated for 5 min at 37 °C to form the open complexes and transferred to room temperature, and ATP and GTP were added to a final concentration of 25 μM. After a 10-min incubation, reactions were washed three times with 1.5 ml of transcription buffer as described (13) and left in a ~20-μl volume. α-[^{32}P]CTP (3000 Ci/mmol, NEN Life Science Products) was added to a final concentration of 0.3 μM, and the incubation was continued for 10 min. After washing, the immobilized EC^{12} was UV-irradiated with a hand-held lamp at 254 nm for 3 min. The lamp was positioned flat at the top of open Eppendorf tubes that contained the reaction mixtures and that were kept on ice. After irradiation, EC^{12} was desorbed from the solid support by addition of imidazole to 100 mM, an equal volume of SDS-containing Laemmli loading buffer (20) was added, and proteins were separated by SDS-PAGE.

In protein-RNA cross-linking experiments in the presence of GreB, immobilized EC^{20} containing radioactively labeled RNA was prepared and used to prepare EC^{21} with 4-thio-UTP instead of UTP. Derivatized EC^{21} was washed with transcription buffer lacking $MgCl_2$ and desorbed from Ni^{2+}-NTA agarose by the addition of 100 mM imidazole. Recombinant GreB (a generous gift of Arun Malhotra, University of Miami) was added to reaction aliquots followed by UV-irradiation as described above. Reaction products were then resolved by SDS-PAGE and visualized by autoradiography.

In Vitro Transcription—To determine transcription elongation rates, elongation complexes stalled at position +20 were prepared in 50 μl of transcription buffer containing 25 μl of Ni^{2+}-NTA agarose, 20 nM of T7 A1 promoter DNA fragment described above, 40 nM RNAP, 0.5 mM ApU, 50 μM CTP and GTP, 2.5 μM [α^{32}P]ATP (300 Ci/mmol). Reactions were incubated for 15 min at 23 °C and were washed as described above. Washed EC^{20} was synchronously started by making reactions 2.5 μM with NTPs. Reactions proceeded for 0–600 s at 23 °C. Reactions were terminated by the addition of formamide-containing loading buffer. To determine transcription termination efficiencies, EC^{20} was restarted by the addition of 250 μM NTPs. Reactions proceeded for 1 min at 23 °C. Products were analyzed by urea-PAGE electrophoresis (7 M urea, 6% polyacrylamide), followed by autoradiography and PhosphorImager analysis.

Transcript Cleavage—Purified immobilized elongation complexes were briefly washed with 1 ml of transcription buffer, pH 9.0. Reactions were left in ~50 μl and incubated at room temperature. At various time points, reaction aliquots were withdrawn, combined with an equal volume of formamide-containing loading buffer, and analyzed by denaturing gel-electrophoresis and autoradiography. Cleavage with GreB was done as described earlier (21).

RESULTS

Deletion Mutagenesis of the Hypervariable Region of E. coli rpoC and Mapping of mAb Binding Epitopes—Alignment of the amino acid sequence of *E. coli* β′ with homologues from other organisms reveals a long region of primary sequence (*E. coli* residues 941–1131) that is present in proteobacteria but is totally absent in homologues from other eubacteria, archaea, and eukaryotes (Fig. 1). In contrast, a much longer sequence (up to 900 amino acids) is found in the corresponding region of β′ subunits from cyanobacteria and chloroplasts. On the N terminus of this hypervariable region is highly conserved segment G (residues 912–940). C-terminal to the hypervariable region is a short segment of conserved sequence that we will refer to as segment G′ (residues 1132–1148; Fig. 1). Segments G and G′ form one continuous stretch of conserved amino acids in eukaryotes, archaea, and most bacteria. Sequence C-terminal to G′ is not conserved and is followed by the C-terminal conserved segment H (residues 1324–1362).

We probed the functional role of the hypervariable region by deletion mutagenesis of the cloned *E. coli rpoC* gene. A linker insertion mutation and a set of limited deletions were obtained as described under "Materials and Methods" and are shown above the alignment in Fig. 1. Δ(941–1130) removed all of the *E. coli* hypervariable region and thus resembles the β′ subunit from *Mycobacterium leprae* (22). Δ(1131–1155)S removed all of segment G′ and replaced it with a Ser residue; Δ(877–948) (not

[2] A. Mustaev and A. Goldfarb, manuscript in preparation.

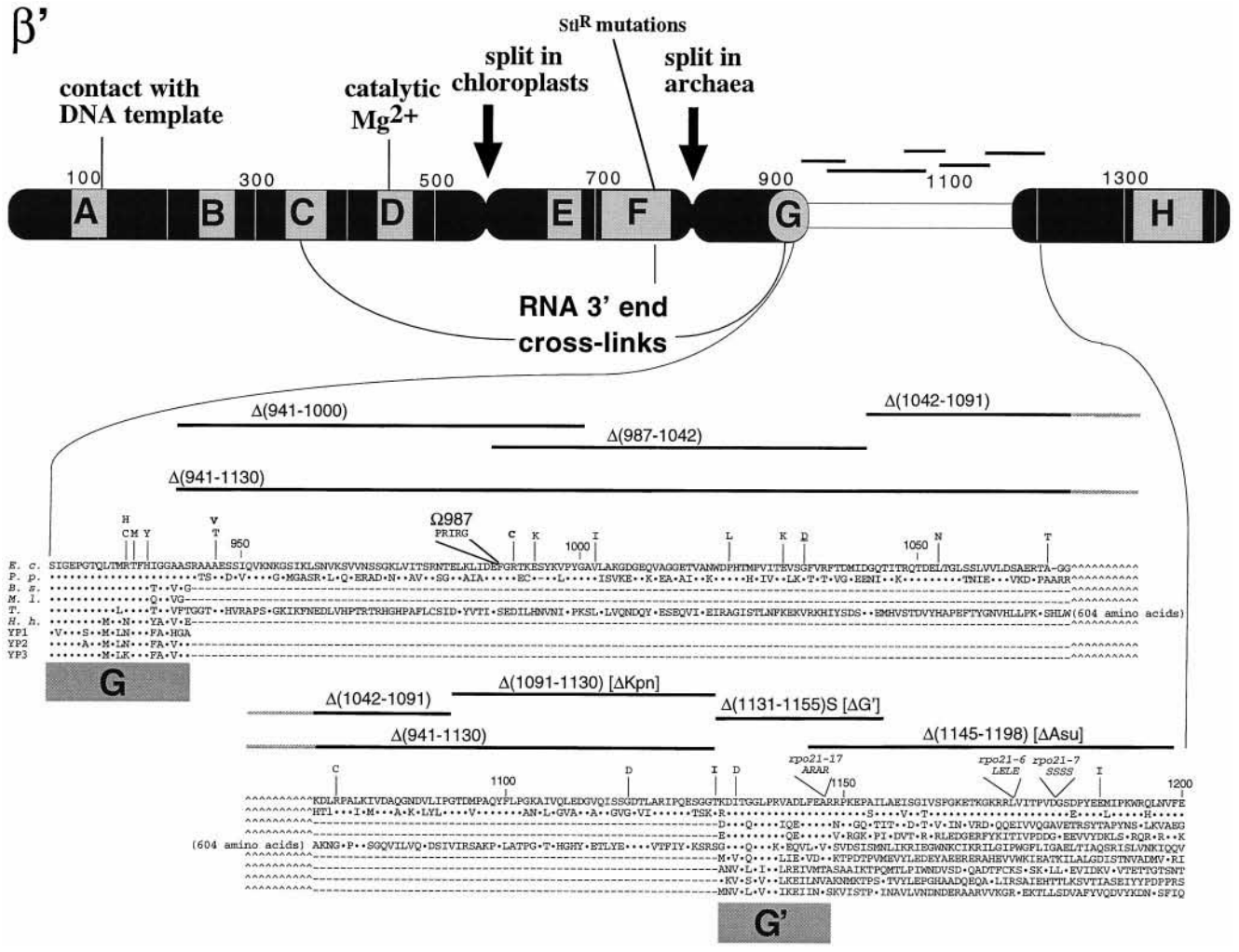

FIG. 1. **Genetic context of the hypervariable region in *E. coli* β′.** The 1407-amino acid-long β′ subunit is represented by the *heavy bar,* with *shaded areas* corresponding to the highly conserved sequence segments, designated *A–H*. The locations of the streptolydigin-resistant mutations (13), residues involved in coordination of the catalytic Mg^{2+} ion (4), residues contacting the template DNA downstream of the catalytic center (29), and sites of cross-linking to the 3′-end of the nascent RNA are also shown (31). The hypervariable region under study is shown by the *white box* and is expanded underneath. In the alignment, the top *E. coli* (*E. c.*) sequence is aligned with the corresponding regions from *P. putida* (*P. p.*), *Bacillus subtilis* (*B. s.*), *M. leprae* (*M. l.*), chloroplasts from tobacco (*T.*), *Halobacterium halobium* (*H. h.*), and yeast RNA polymerases I, II, and III (YP1, YP2, and YP3, respectively). Deletions obtained in this work are shown as *black bars*. In addition, point mutations altering *E. coli* RNAP termination properties *in vivo* (24) (*plain text*), suppressing the *nusA134* allele (33) (*boldface type*), and affecting chromosomal replication control (38) (*underlined*), as well as insertional mutations in the homolog from yeast RNAP II altering interactions with TFIIS (35) (*italicized*) are also shown above the *E. coli* sequence.

shown in Fig. 1) deleted conserved segment G. Δ(1145–1198) removed 54 amino acids immediately C-terminal to G′. Δ*(1145–1198)* removed coding sequences between in-frame naturally occurring recognition sites of restriction endonuclease *Asu*I and is referred to as Δ*Asu* throughout the text. Similarly, Δ*(1091–1130)* removed coding sequences between the in-frame naturally occurring *Kpn*I sites and is referred to as Δ*Kpn*.

Previously, one of us reported the isolation of two anti-β′ mAbs, Pyn1 and Pyn4, using RNAP core enzyme as an antigene (15). Pyn1 efficiently inhibited transcription by *E. coli* RNAP as well as by the *Pseudomonas putida* enzyme,[3] whereas Pyn4 had no effect on transcription (15). We localized Pyn1 and Pyn4 binding epitopes using the β′ deletion mutants described above. To locate mAb binding epitopes, cells expressing different plasmid-borne variants of *rpoC* were induced and lysed, and proteins were separated by SDS-PAGE, followed by Western blotting with Pyn1 or Pyn4. As shown in Table I, all deletions in the hypervariable region abolished Pyn1 binding and thus must have destroyed the binding epitope. In contrast, Δ*(877–948)*, Δ*(1131–1155)S*, and Δ*Asu* did not affect Pyn1 binding. These data suggest that β′ amino acids 949–1091 contain the Pyn1 binding epitope. However, because both Δ(941-1000) and ΔKpn—Δ(1091-1130), which are 90 amino acids apart, disrupt Pyn1 binding, the antibody epitope may be conformational rather than linear. Thus, we can not exclude that β′ sequences outside the hypervariable region may also participate in the binding of this inhibitory antibody.

Δ*Asu* was the only deletion that abolished the binding of Pyn4. We conclude that β′ amino acids 1145–1198 contribute to Pyn4 binding epitope**.**

Properties of rpoC Mutants in Vivo—All *rpoC* deletions were obtained in pMKa201*S693F rpoC* expression plasmid. In this plasmid, a transdominant streptolydigin-resistant *S693F* allele of *rpoC* is placed under the control of the inducible *lac* promoter (14). Therefore, the function of mutant, plasmid-borne *rpoC* can be tested *in vivo* by registering its ability to confer streptolydigin resistance to the sensitive host cells CAG 14064 (13). When CAG 14064 cells overproducing the WT and

[3] A. Lebedev and V. Nikiforov, unpublished results.

TABLE I
Properties of rpoC mutants

Allele	Stl[a]	*rpoC*^{ts} suppression[b]	Assembly[c]	Pyn1[d]	Pyn4[d]
Wild type	−	+	+[e]	+	+
S693F	+	+	+[e]	+	+
Ω987	+	+	+	+	+
Δ(877–948) [ΔG]	−	−	−	+	+
Δ(941–1130)	−	−	−[e]	−	+
Δ(941–1000)	−	+/−	+	−	+
Δ(1042–1091)	−	+/−	+	−	+
Δ(1091–1130) [ΔKpn]	−	+/−	+[e]	−	+
Δ(1131–1155)S [ΔG′]	−	−	−[e]	+	+
Δ(1145–1198) [ΔAsu]	−	+	+[e]	+	−

[a] Colony formation by CAG14064 (13) host strain on LB plates containing 100 μg/ml ampicillin, 12.5 μg/ml streptolydigin, and 1 mM IPTG.

[b] Colony formation by RL602 (25) host strain at 42 °C on LB plates containing 100 μg/ml ampicillin and 1 mM IPTG.

[c] RNAP assembly was monitored *in vitro* by the appearance of characteristic peaks during chromatographic purification of reconstitution mixtures (17) and transcriptional activity.

[d] Cells expressing the indicated plasmid-borne variants of *rpoC* were induced, and proteins were separated by SDS-PAGE, followed by Western blotting with Pyn1 or Pyn4.

[e] Indicates cases in which experiments to purify mutant RNAPs from cell extracts by affinity chromatography on Ni^{2+}-NTA agarose were performed. The results of the *in vitro* and *in vivo* assembly assays were always in agreement.

mutant β′ subunits were plated on a medium containing 12.5 μg/ml streptolydigin, only cells overproducing parental S693F β′, and the linker insertion Ω987 formed colonies (Table I).

In another test of the *in vivo* function of mutant *rpoC* genes, the RL602 *E. coli* cells were transformed with pMKa201*S693F* and its derivatives, and plated at 42 °C. RL602 cells harbor an amber mutation in the chromosomal copy of *rpoC* that is suppressed by a temperature-sensitive suppressor (23). RL602 grows at 30 °C but fails completely to grow at 42 °C. Cells overproducing S693F β′, as well as Ω987, Δ(1042–1091), Δ(941–1000), Δ(987–1042), ΔKpn, and ΔAsu formed colonies at the elevated temperature (data not shown). Cells overproducing S693F β′, Ω987, and ΔAsu grew robustly at 42 °C, whereas the others formed minute colonies (Table I).

We do not know whether the mutant β′ subunits were the only source of β′ at high temperature. Landick *et al.* (24) encountered similar "partial" phenotypes when testing *in vivo* function of mutant, plasmid-borne *rpoB* genes. These authors suggested that growth at restrictive temperature may occur when the plasmid-borne *rpo* gene provides enough partially functional RNAP to allow the growth of the host, which has a low level of the wild-type, chromosomally encoded RNAP even at restrictive temperature. In contrast, administering streptolydigin completely inhibits wild-type, chromosomal RNAP, and thus prevents the cell growth.

In Vitro Reconstitution of Mutant RNAPs—Because the results of functional assays *in vivo* were inconclusive, we assembled mutant β′ into RNAP *in vitro*. Assembled RNAP forms characteristic peaks during chromatography on Superose-6 and Mono Q columns (17). No such peaks were observed in the course of purification of reconstitution mixtures containing Δ(877–948), Δ(1131–1155)S, and Δ(941–1130) and WT α, β, and σ subunits; neither crude reconstitution mixtures nor chromatographic fractions contained any RNAP activity (Table I and data not shown).

The β′ subunits expressed from pMK201 plasmid are fused to the C-terminal His_6 tag, allowing easy purification of RNAP harboring plasmid-borne β′ (13). Our repeated attempts to purify RNAPs harboring the two largest β′ deletions from cells using affinity chromatography failed (data not shown). We conclude that deletions of conserved segments G and G′, as well as removal of the entire hypervariable region, completely abolish the ability of β′ to enter *E. coli* RNAP core *in vitro* and *in vivo*.

5 smaller deletions (Δ(941–1000), Δ(987–1042), Δ(1042–1091), ΔKpn and ΔAsu) assembled into RNAP *in vitro* as judged by the appearance of characteristic chromatographic peaks in the course of purification. The catalytic proficiency of RNAP mutants was demonstrated by template-dependent affinity labeling of shortened β′ polypeptides with derivatized nascent RNA. In this reaction, Ni^{2+}-NTA agarose-immobilized RNAP was used to form open complexes with the T7 A1 promoter-containing DNA fragment. Transcription was primed with a derivatized, photoactive ApUpC, complimentary to positions +1–+3 of the promoter. In the presence of unlabeled GTP and ATP, transcription proceeded to position +11 and was halted because of the absence of CTP, specified by the position +12 of the template. After extensive washing, elongation complexes stalled at position 11 (EC^{11}) were extended with radioactive CTP to obtain EC^{12}. EC^{12} containing radioactive and photoactive RNA was washed and UV-irradiated to induce protein-RNA cross-link formation, and the reaction products were separated by SDS-PAGE. Irradiation of $RNAP^{WT}$ elongation complexes resulted in radioactive labeling of both β and β′ with equal efficiency (Fig. 2*A*). As can be seen from the autoradiogram presented on Fig. 2*A*, labeled, full-sized β′ is absent from lanes containing mutant enzymes, establishing that little or no contaminating $RNAP^{WT}$ was present. Instead, lanes containing mutant enzymes have a labeled band with the mobility of β, which represents a mixture of labeled full-sized β and mutant β′ subunits (full-sized β′ and β are 1407 and 1342 amino acids long, respectively; deletions in β′ make it impossible to separate the two proteins by SDS-PAGE). Control experiments established that (*i*) subunit labeling was template-dependent, and (*ii*) subunit labeling did not occur when photoactive, radioactive RNA 12-mer was added to RNAP *in trans*. Furthermore, cleavage of the RNA-product adduct with formic acid demonstrated that the RNA moiety of the adduct was 12 nucleotides in length (data not shown).[2] On the basis of these results, we conclude that the mutant enzymes are assembled, active, and free of contaminating $RNAP^{WT}$.

Transcription by Mutant RNA Polymerases—We decided to concentrate on $RNAP^{\Delta Kpn}$ and $RNAP^{\Delta Asu}$ because preliminary experiments showed that $RNAP^{\Delta(941–1000)}$, $RNAP^{\Delta(987–1042)}$, and $RNAP^{\Delta(1042–1091)}$ are very similar to $RNAP^{\Delta Kpn}$.

Weilbaecher *et al.* (25) reported that point mutations in the β′ region under study altered the elongation and termination properties of RNAP *in vivo* and *in vitro*. Accordingly, we checked the transcription elongation and termination properties of mutant RNAPs. Immobilized elongation complexes stalled at position 20 of the T7 A1 promoter-driven transcription unit were prepared. To determine elongation rates, transcription was resumed by the addition of NTPs at subsaturating (2.5 μM) concentration. At various time points, reaction aliquots were withdrawn, and the products were analyzed by denaturing PAGE (Fig. 2*A*). As can be seen from Fig. 2, $RNAP^{\Delta Asu}$ did not differ significantly from $RNAP^{WT}$ in this assay, but $RNAP^{\Delta Kpn}$ was dramatically "slower." The apparent slow rate of transcript elongation by $RNAP^{\Delta Kpn}$ was caused by extended (t[ifrax;1/2] ~ 2.5 min) pausing at template positions 26 and 27, and later at positions 37 and 56. The same pausing pattern was obtained when transcription by immobilized $RNAP^{\Delta Kpn}$ was resumed from positions 12, 23, and 25 (data not shown).

Extended pausing by $RNAP^{\Delta Kpn}$ at positions 26, 27, and 56 is intriguing, because transcription complexes artificially stalled

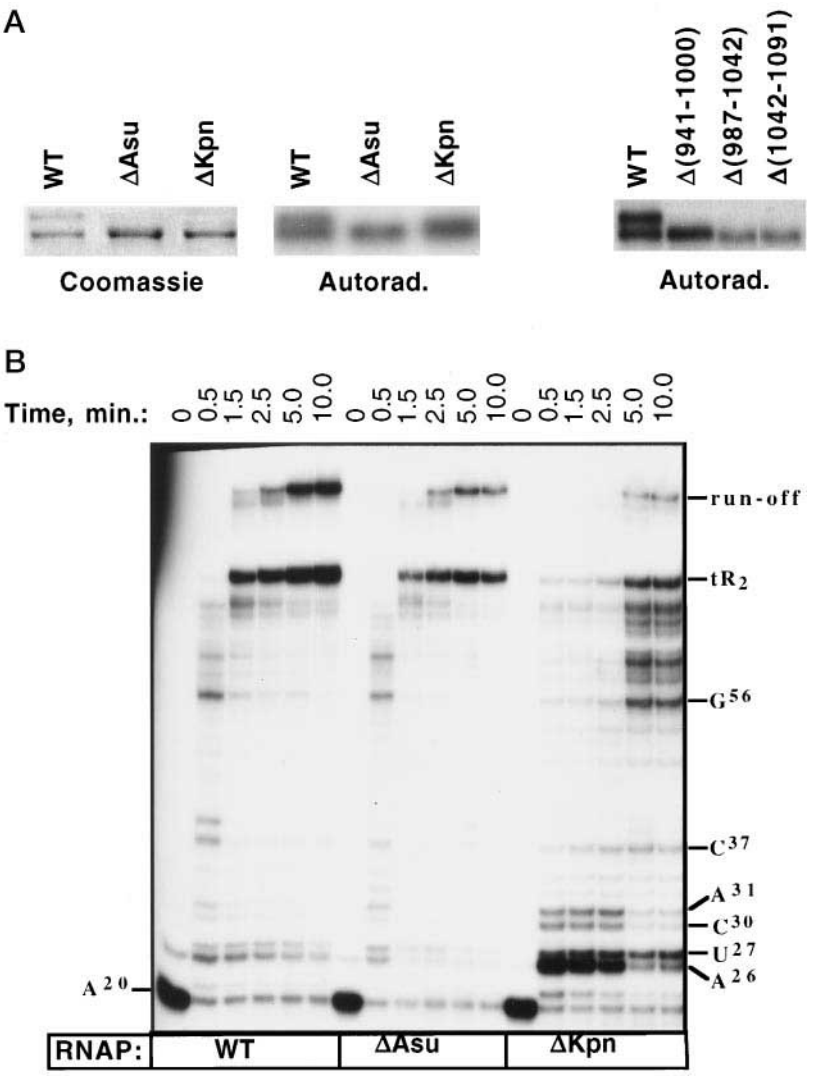

FIG. 2. ***In vitro* transcription by mutant enzymes.** *A,* RNA-protein photocross-linking in EC^{12} formed by mutant RNAPs. Immobilized EC^{12} formed by the indicated RNAPs and containing photoactivatable, cross-linkable nascent RNA was UV-irradiated, and the reaction products were resolved on the 4% SDS-polyacrylamide gel, stained, and visualized by autoradiography. *B,* transcript elongation at subsaturating NTP concentration. EC^{20} were prepared using template 1 of Nudler *et al.* (19), containing the T7 A1 promoter and λ tR2 terminator. Transcription was resumed by the addition of NTP to 2.5 μM. Reactions proceeded for the times indicated, and reaction products were analyzed by 6% urea-PAGE followed by autoradiography. RNA in the indicated paused complexes was sized using artificially stalled elongation complexes with RNA of defined length as markers.

at these positions are efficiently converted into an arrested conformation (26–30). During arrest at EC^{26} or EC^{27}, the catalytic center of the enzyme disengages from the 3′-end of the nascent RNA, and RNAP slides backward. As a result, the catalytic center repositions to about position 20. This intermediate complex is still able to continue transcription by sliding forward to the active conformation; it can also slide back even further, to position 11, and become permanently arrested. The permanently arrested, dead-end complex can only be rescued by transcript cleavage. In the presence of the transcript cleavage factor GreB, the catalytic center hydrolyses the RNA at position 11. The newly generated 3′-end of the 5′-end-proximal, 11-mer cleavage product can then be elongated by RNAP; the 3′-end-proximal cleavage products are lost from the complex.

To investigate the nature of the $RNAP^{\Delta Kpn}$ pause at position 26, immobilized EC^{20} was incubated for 2 min in the presence of low (2.5 μM) concentrations of NTPs, followed by a brief (30 s) incubation with GreB (Fig. 3*A*). As can be seen, addition of GreB to transcription reaction resulted in the appearance of new products. These new cleavage products were stably associated with transcription complexes (data not shown) and had the electrophoretic mobility of 20- and 22-mers. Control lanes of Fig. 3*A* demonstrate that the addition of GreB to stalled, arrested $RNAP^{\Delta Kpn}$ EC^{27} resulted in cleavage, generating a 5′-terminal 11-mer, as expected. Based on these data, we conclude that in paused $RNAP^{\Delta Kpn}$ EC^{26} and EC^{27}, the transcript has reversibly slid out of the active site, and therefore, the paused complexes correspond to intermediate of the arrested complex formation pathway (28–30).

Increased pausing by $RNAP^{\Delta Kpn}$ could be explained by its increased ability to slide backward at certain parts of the template. Although the ability to slide back is difficult to test, we investigated the efficiency of EC^{27} arrest complex formation by $RNAP^{\Delta Kpn}$. In this experiment, shown in Fig. 3*B* by the extent of transcription arrest by artificially stalled, purified $RNAP^{\Delta Kpn}$ EC^{27} was determined by the ability to be chased into EC^{32} upon the addition of ATP and CTP. Freshly purified EC^{27} formed by both $RNAP^{WT}$ and $RNAP^{\Delta Kpn}$ were elongation competent (Fig. 3*B*, *lanes 2* and *5*). However, after 5 min of incubation at 37 °C in the absence of nucleotides only 10% of initial EC^{27} could be chased upon addition of nucleotides. Importantly, there was no difference between $RNAP^{\Delta Kpn}$ and $RNAP^{WT}$ in the extent of arrest (Fig. 3*B*, *lanes 3* and *6*).

Extensive pausing by $RNAP^{\Delta Kpn}$ could be caused by an unusually high apparent K_m for the incoming UTP (corresponding to position 27), accompanied by reversible sliding to position 20. Indeed, increasing NTP concentration decreased pausing by $RNAP^{\Delta Kpn}$. At high (250 μM) substrate concentrations, $RNAP^{\Delta Kpn}$ completed a single round of transcription in 1 min and terminated transcription on the λ tR2 terminator with nearly the same efficiency as $RNAP^{WT}$ and $RNAP^{\Delta Asu}$ (Fig. 3*C*).

Transcript Cleavage by Mutant RNAPs—A genetic screen of yeast RPO21 (an evolutionary homologue of *rpoC*) identified mutations that altered the ability of RNAP II to interact with

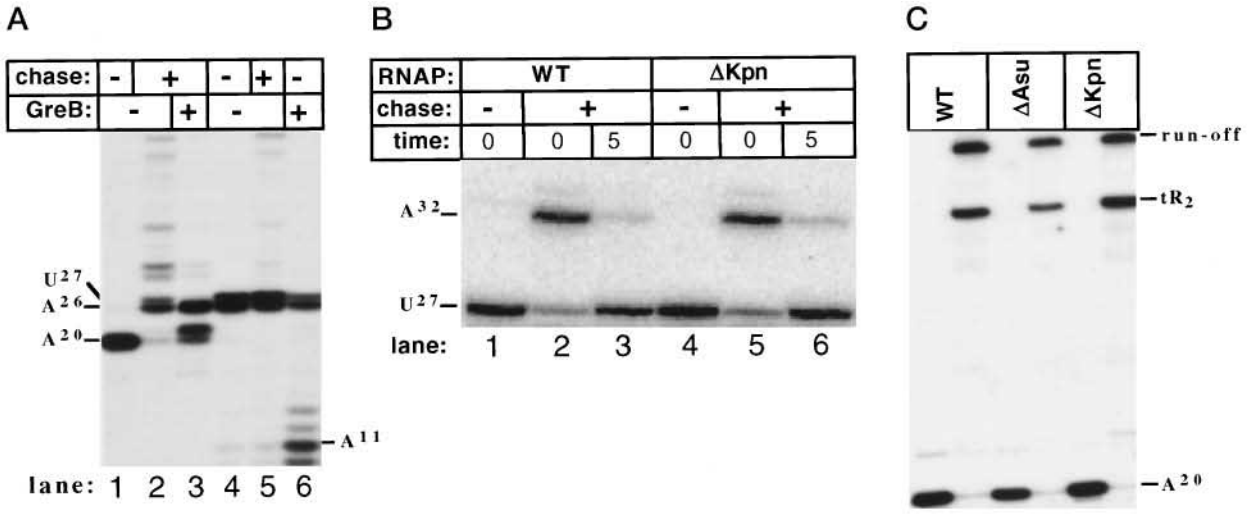

FIG. 3. **The mechanism of pausing defect of RNAP$^{\Delta Kpn}$.** *A,* transcription elongation in the presence of GreB. Immobilized RNAP$^{\Delta Kpn}$ EC^{20} (*lane 1*) was restarted by the addition of 5 μM NTP, and reaction was allowed to proceed for 2 min (*lane 2*). At this point, 400 ng of recombinant GreB was added, followed by additional 30 s of incubation (*lane 3*). Stalled EC^{27} (*lane 4*) was supplemented with 5 μM NTP, incubated for 2 min (*lane 5*), and treated with GreB for additional 30 s (*lane 6*). An autoradiograph of 15% urea polyacrylamide gel is presented. *B,* arrested complex formation by RNAP$^{\Delta Kpn}$ and RNAP^{WT}. Stalled EC^{27} was prepared (*lanes 1* and *4*) and immediately restarted by the addition of 10 μM of ATP and CTP (*chase*) to allow the formation of EC^{32} (*lanes 2* and *5*). Alternatively, EC^{27} was incubated for 5 min at 37 °C, followed by the addition of NTP (*lanes 3* and *5*). Reaction products were analyzed as in *A*. *C,* transcription termination at λ tR2 terminator. Elongation by purified EC^{20} was resumed by the addition of 250 μM NTP. Reactions proceeded for 1 min at 23 °C. Products were analyzed on a 6% urea gel.

transcript cleavage factor TFIIS (31). Seven mutations were isolated and they all clustered between conserved segments G and H (32). It was subsequently shown that these mutations inhibited interaction of mutant RNAP II with TFIIS by as much as 50-fold (33). Because these mutations occurred very close to hypervariable region studied here (see Fig. 1), we investigated the transcript cleavage activity of mutant *E. coli* RNAPs. As can be seen from Fig. 4*A*, EC^{21} formed by RNAP$^{\Delta Kpn}$ required approximately 10 times more GreB to achieve the same extent of cleavage as complexes formed by RNAP^{WT} and RNAP$^{\Delta Asu}$. The same result was obtained when the GreB homolog GreA was used to induce the cleavage reaction (data not shown).

When EC^{20} formed by RNAP^{WT} was incubated in pH 9.0 buffer (a condition known to stimulate the intrinsic nucleolytic activity of RNAP (21)) transcript cleavage was observed (Fig. 4*B*). After 5 min incubation in pH 9.0 buffer, >75% of RNAP^{WT} and RNAP$^{\Delta Asu}$ EC^{20} had undergone cleavage (Fig 4*B, lanes 2* and *6*, respectively). In contrast, only 10% of RNAP$^{\Delta Kpn}$ EC^{20} had undergone cleavage after a 5-min incubation, and less than 60% was cleaved after a 20-min incubation in pH 9.0 buffer (lanes 10 and 12). To estimate GreB binding to RNAP$^{\Delta Kpn}$, we performed UV-photo-cross-linking of GreB to derivatized 3′-end of nascent RNA in RNAP^{WT} and RNAP$^{\Delta Kpn}$ EC^{21} (Fig. 4*C*). In agreement with previous data (36, 39), β′ and GreB were efficiently cross-linked to derivatized, radioactive RNA. Lowering the amount of GreB in the reaction resulted in decreased cross-linking of GreB to RNA, but the amount of β′-RNA cross-link remained constant. As can be seen from Fig. 4*C*, RNAP$^{\Delta Kpn}$ complexes required approximately 10 times more GreB to achieve the same extent of GreB-RNA cross-links as complexes formed by RNAP^{WT}. This effect was especially evident at low GreB concentrations (compare Fig. 4*C*, *lanes 6* and *12*). From this result, we conclude that ΔKpn either directly decreases GreB binding to RNAP or alters the relative position of GreB and the RNA 3′-end, thus decreasing the efficiency of GreB-RNA cross-linking near the catalytic center.

To estimate GreB binding to mutant RNAP directly, we used GreB protein tagged with an N-terminal heart muscle protein kinase (HMPK) recognition site.[4] Different amounts of ^{32}P-end-labeled HMPK-GreB were combined with RNAP^{WT} or RNAP$^{\Delta Kpn}$ core enzymes, and after a short incubation to allow complex formation, the reaction products were resolved by native PAGE and GreB-containing complexes were visualized by autoradiography (Fig. 4*D*). As can be seen, both enzymes formed complexes with [^{32}P[HMPK-labeled GreB with the same efficiency.

Effects of mAb Binding to RNAP on Transcription in Vitro—In agreement with our previous data (15), mAb Pyn1 efficiently inhibited elongation of the nascent RNA from EC^{20} to EC^{23} by RNAP^{WT} (Fig. 5*A, top, lane 3*). Transcription by RNAP$^{\Delta Kpn}$ was unaffected by Pyn1 (Fig. 5*A, top, lane 7*), because Pyn1 did not bind RNAP$^{\Delta Kpn}$ (Fig. 5*A, bottom, lane 5*). In contrast, Pyn4 had no effect on EC^{20} to EC^{23} conversion by both enzymes, even though more than 50% of elongation complexes were bound to mAb at the experimental conditions used (*lanes 3* and *6*).

Pyn1 completely inhibited intrinsic transcript cleavage by RNAP^{WT} at pH 9.0 (Fig. 5*B, lanes 6* and *7*). Transcript cleavage by RNAP$^{\Delta Kpn}$ was unaffected at these conditions (data not shown). When GreB was added to RNAP^{WT}, EC^{20} transcript cleavage occurred even in the presence of Pyn1 (Fig. 5*C*). Still, an ~10-fold excess of GreB was required in the presence of Pyn1 to achieve the same extent of cleavage as in its absence (compare Fig. 5*C, lanes 5* and *7*). GreB did not cause dissociation of Pyn1 from RNAP, as the experiment shown in Fig. 5*D* demonstrates. In this experiment, different amounts of ^{32}P-end-labeled HMPK-GreB were combined with RNAP^{WT} core in the presence or the absence of Pyn1. After a short incubation to allow complex formation, the reaction products were resolved by native PAGE, and GreB-containing complexes were visualized by autoradiography. In the absence of Pyn1, [^{32}P[HMPK-GreB formed a complex with RNAP (Fig. 5*D, lanes 1–3*). Addition of Pyn1 resulted in the appearance of a radioactive complex with a slower electrophoretic mobility (*lanes 4–6*). We

[4] N. Loizos, unpublished results.

FIG. 4. **Transcript cleavage by mutant RNA polymerases.** *A,* EC^{21} containing RNA radioactively labeled at U^{21} was desorbed from Ni^{2+}-NTA agarose with 50 mM imidazole (*lanes 1, 5,* and *9*) and supplemented with GreB (*lanes 2, 6,* and *10,* 0.04 ng; *lanes 3, 7,* and *11,* 0.4 ng; *lanes 4, 8,* and *12,* 4 ng). Reactions were incubated for 5 min, and products were resolved by denaturing PAGE in 10% urea-gel. *B,* intrinsic transcript cleavage at elevated pH. Immobilized EC^{20} was transferred into a pH 9.0 transcription buffer, and reactions were incubated for indicated times, followed by electrophoresis and autoradiography. *C,* RNA-protein photo-cross-linking. EC^{21} formed by $RNAP^{WT}$ and $RNAP^{\Delta Kpn}$ was UV-irradiated in the absence (*lanes 1* and *7*) or in the presence of decreasing concentrations of GreB (*lanes 2* and *8*, 400 ng; *lanes 3* and *9,* 40 ng; *lanes 4* and *10*, 4 ng; *lanes 5* and *11*, 0.4 ng; *lanes 6* and *12,* 0.04 ng). Reaction products were resolved on the 4–20% gradient SDS-gel and visualized by autoradiography. *D,* binding of $RNAP^{WT}$ and $RNAP^{\Delta Kpn}$ to [^{32}P]HMPK-GreB. 1 μg of RNAP of the indicated core enzymes was combined with increasing concentrations of [^{32}P]HMKP-GreB. Reactions were incubated for 10 min to allow the complex formation, resolved by native PAGE on a 4–15% Phast gel, and visualized by autoradiography.

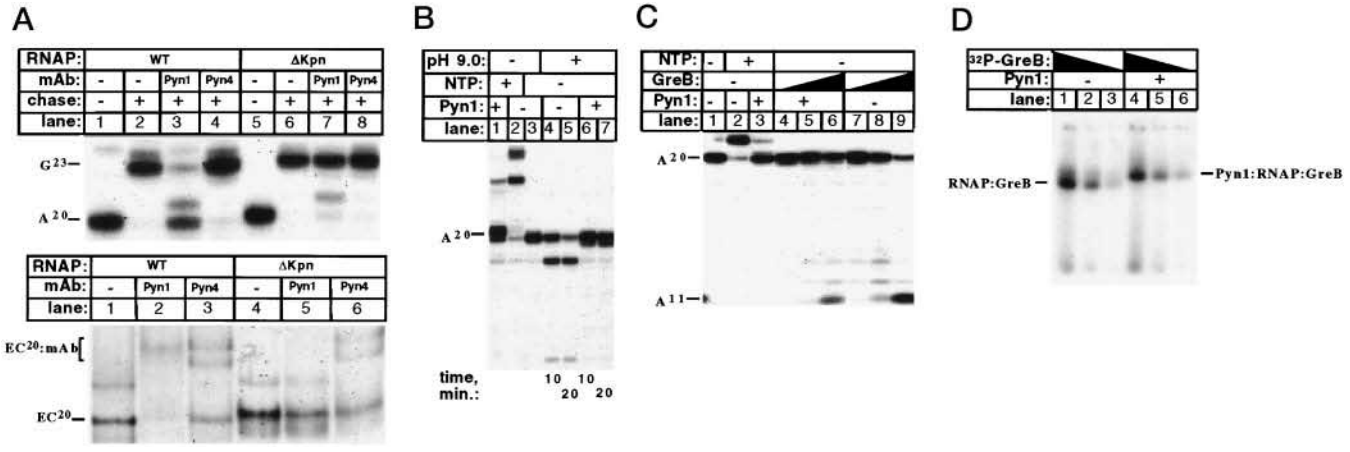

FIG. 5. **Effects of mAb binding on transcription *in vitro*.** *A,* EC^{20} containing radioactively labeled RNA were desorbed from Ni^{2+}-NTA agarose with 50 mM imidazole (*lanes 1* and *5, top panel*, and *lanes 1* and *4, bottom panel*). Reactions were then supplemented with the indicated mAbs and 10 μM ATP and CTP (*chase*) to allow elongation to position 23. Reaction products were resolved by denaturing PAGE in 10% urea-gel (*top panel*) or by native PAGE in 4% gel (*bottom panel*). *B,* intrinsic transcript cleavage at elevated pH. Immobilized EC^{20} was transferred into a pH 9.0 transcription buffer, and reactions were incubated for indicated times in the presence or in the absence of Pyn1, followed by electrophoresis and autoradiography. *C,* EC^{20} formed by $RNAP^{WT}$ was treated with increasing concentrations of GreB in the presence or in the absence of Pyn1, and reaction products were resolved on a 15% denaturing gel, visualized by autoradiography. In *B* and *C, lanes 1* and *2* are controls, demonstrating that Pyn1 efficiently inhibited transcript elongation at the conditions used. *D,* binding of RNAP to [^{32}P]HMPK-GreB. RNAP core enzyme was combined with increasing concentrations of [^{32}P]HMKP-GreB in the presence (*lanes 4–6*) or the absence (*lanes 1–3*) of Pyn1. Reactions were incubated for 10 min to allow the complex formation and resolved by native PAGE on a 4–15% Phast gel.

conclude that GreB and Pyn1 can simultaneously bind to the RNAP core molecule.

DISCUSSION

A set of deletions in the cloned *E. coli rpoC* gene was constructed to evaluate the role of an evolutionarily hypervariable region of the RNAP β′ subunit (amino acids 941–1130) in enzyme function. This region is completely absent from β′ subunits of most bacteria and is highly divergent within proteobacteria (Fig. 1). Suprisingly, deletion of the entire hypervariable region completely prevented RNAP assembly both *in vivo* and *in vitro*. Obviously, similar deletions (relative to *E. coli* β′) naturally found in the β′ subunits from other bacteria do not prevent RNAP assembly in these organisms. Apparently, compensating differences in the α, β, and/or β′ subunits of these bacteria allow RNAP assembly to proceed.

The five functional deletions obtained in this work together remove 243 amino acids (>17%) of β′ and prove that, as in β, long regions of β′ sequence are dispensable for basic functions of *E. coli* RNAP *in vitro*. These functional deletions clearly fall into two classes. ΔAsu removes 54 amino acids N-terminal of the hypervariable region and does not change RNAP transcription *in vitro*. In contrast, deletions of similar size spanning the hypervariable region (Δ941–1000, Δ987–1042, Δ1042–1091, and Δ1091–1130 (ΔKpn)) cause a dramatic defect in transcription elongation at subsaturating substrate concentrations and inhibit transcript cleavage.

The functional difference between the two classes of mutants is also evident from different effects of mAb binding. Pyn1 binds to the hypervariable region (amino acids 948–1130) and efficiently inhibits RNA synthesis and intrinsic transcript cleavage. In contrast, Pyn4, the binding epitope of which is destroyed by ΔAsu, has no effect on transcription. The hypervariable region is highly immunogenic: in an independent study Luo and Krakow (34) isolated several mAbs that interacted with this region of *E. coli* β′. mAb 311G2 inhibited RNA synthesis by interfering with substrate binding, and its binding epitope was within β′ amino acids 1047–1093. Thus, 311G2 must be very similar to Pyn1.

The most striking feature of $RNAP^{\Delta Kpn}$-like enzymes is prolonged pausing at sites of transcriptional arrest (26–30), suggesting that the hypervariable region is involved in transcript elongation and cleavage. However, this involvement is proba-

bly indirect, because the hypervariable region is completely absent from RNAP of most organisms. We therefore propose that the deletions in β′ studied here act indirectly, by affecting function(s) of adjacent conserved segments. There is good evidence that segment G, which is located immediately to the N terminus of the hypervariable region, participates directly in transcript cleavage and transcriptional arrest. Borukhov *et al.* (35) demonstrated that an 80-amino acid-long β′ fragment containing the 8 C-terminal-most amino acids of conserved segment G and the 74 N-terminal-most amino acids of the hypervariable region contains the site that is cross-linked to the 3′-end of the nascent RNA in EC^{20}. It was later found that this protein-RNA contact is indicative of the arrested conformation of the elongation complex (40). Further protein-RNA cross-linking experiments established that segment G *and* GreB proteins could both be cross-linked to the nascent RNA 3′-terminus and thus must be within several Å of each other in the complex (36). Thus, it is likely that segment G can form an alternative, unproductive RNA binding site during transcript elongation. The defect in $RNAP^{\Delta Kpn}$-like enzymes could be the result of increased interactions between region G and the RNA 3′-end in the mutant complex at the potential arrest sites, causing backsliding, and elevated apparent K_m for the incoming nucleoside triphosphate. This defect is only observed at subsaturating substrate concentrations, because at high substrate concentrations, addition of NMP to the 3′-end of the nascent RNA occurs faster than backsliding, and mutant enzymes elongate RNA normally. Close inspection of the gel shown in Fig. 2*B* reveals that $RNAP^{WT}$ also pauses at the sites of transcriptional arrest, but clears the pause sites rapidly. Thus, reversible backsliding may play a role in $RNAP^{WT}$ pausing as well.

One of the goals of this study was to obtain RNAP mutants defective in interactions with transcript cleavage factors. Data of Wu *et al.* (33) suggested that the region of the largest (β′-like) subunit of yeast RNAP II between conserved segments G and H may form the primary site of TFIIS interactions with its target RNAP. Seven tightly clustered linker insertion mutants studied by these authors showed little or no effect in intrinsic transcript cleavage and transcription elongation at high NTP concentrations but were defective in the TFIIS-dependent transcript cleavage, and did not form a complex with TFIIS *in vitro*. Three of the seven yeast mutations occurred immediately to the right of conserved segment G′. In *E. coli*, the corresponding amino acids are removed by Δ(1145–1198) (ΔAsu) mutation. Suprisingly, ΔAsu is the least defective of the five functional RNAP mutants obtained in this work. In contrast, ΔKpn-like enzymes with deletions in hypervariable region itself are defective in Gre-dependent transcript cleavage, but the defect is relatively mild. Unlike the situation with yeast RNAP, the interactions between the mutant enzymes and the transcript cleavage factor were not affected as measured by the native gel binding assay. The nature of the cleavage defect is complex, because both the intrinsic transcript cleavage activity of the catalytic center and GreB-RNA cross-linking are affected by mutations. The latter defect could be due to repositioning of segment G, which is known to be close to GreB in the elongation complex (see above). Thus, our data suggest that TFIIS and GreB, which are functional analogs, but not homologous to each other, may interact with their respective RNA polymerases differently.

Published alignments of β′-like RNAP subunits (7, 24) differ significantly from the alignment presented in Fig. 1. The main feature of our alignment is the existence of an additional conserved segment, G′ (*E. coli* positions 1031–1040). Our alignment offers clues to the striking differences in the biochemical properties of mutant enzymes obtained in this work and is supported by the pattern of evolutionary variation in this region. In archaea, eukaryotes, and most bacteria, segments G and G′ are fused, forming one continuous stretch of conserved amino acids. In contrast, in proteobacteria, cyanobacteria, and chloroplasts, a long insertion occurred at the G/G′ boundary (referred to as the hypervariable region in this work). The sequence of this insert appears to be unrelated between proteobacteria and cyanobacteria, and is highly divergent within each group. Interestingly, the site of the insertion relative to the G/G′ boundary is the same in both groups, which are far apart from each other phylogenetically (41). Thus, insertions at the G/G′ boundary may have occurred at least twice in evolution. The inserted region is highly immunogenic, and may therefore loop out at the surface of the RNAP. Deletions in or mAb binding to the hypervariable region may alter the relative position of G and G′, resulting in the observed defects in transcription. The importance of G′ is highlighted by the fact that the smallest deletion obtained in this work, *Δ(1131–1155)S*, which removed G′, failed to assemble in RNAP *in vitro*. On the other hand, it is possible that removal of approximately 50 amino acids C-terminal to G′ in the ΔAsu mutant did not alter the relative positions of G and G′ and thus had no major impact on the transcription properties of RNAP. Ongoing site-specific mutagenesis should clarify the functional role of this segment in RNA polymerase assembly, catalytic function, and transcript cleavage.

Acknowledgments—We are grateful to Arkady Mustaev for reagents and advice on protein-RNA cross-linking, Nick Loizos for the gift of plasmid overproducing HMPK-GreB, and Robert Landick and Cathleen Chan for useful comments and critically reading the manuscript. Part of this work was done by N. Z. during her time at Alex Goldfarb's laboratory (Public Health Research Institute, New York, NY).

REFERENCES

1. Zillig, W., and Gropp, F. (1986) in *RNA Polymerase and the Regulation of Transcription,* (Reznikoff, W. S., Burgess, R. R., Dahlberg, J. E., Gross, C. A., Record, M. T., Jr., and Wickens, M. P., eds) pp. 17–24, Elsevier Science Publishing Corp., New York
2. Gross, C. A., Lonetto, M., and Losick, R. (1992) in *Transcriptional Regulation.* (Yamamoto, K., and McKnight, S., eds) pp. 129–176, Cold Spring Harbor Laboratory, Cold Spring Harbor, NY
3. Mustaev, A., Kashlev, M., Lee, J. Y., Polyakov, A., Lebedev, A., Zalenskaya, K., Grachev, M., Goldfarb, A., and Nikiforov, V. (1991) *J. Biol. Chem.* **266,** 23927–23931
4. Zaychikov, E., Martin, E., Denissova, L., Kozlov, M., Markovtsov, V., Kashlev, M., Heumann, H., Nikiforov, V., Goldfarb, A., and Mustaev, A. (1996) *Science* **73,** 107–109
5. Allison, L. A., Moyle, M., Shales, M., and Ingles, C. J. (1985) *Cell* **42,** 599–610
6. Sweetser, D., Nonet, M., and Young, R. A. (1987) *Proc. Natl. Acad. Sci. U. S. A.* **84,** 1192–1196
7. Pühler, G., Leffers, H., Gropp, F., Palm, P., Klenk, H.-P., Lottspeich, F., Garrett, R. A., and Zillig, W. (1989) *Proc. Natl. Acad. Sci. U. S. A.* **86,** 4569–4573
8. Igarashi, K., and Ishihama, A. (1991) *Cell* **65,** 1015–1022
9. Severinov, K., Kashlev, M., Severinova, E., Bass, I., McWilliams, K., Kutter, E., Nikiforov, V., Snyder, L., and Goldfarb, A. (1994) *J. Biol. Chem.* **269,** 14254–14259
10. Tavormina, P. L., Landick, R., and Gross, C. A. (1996) *J. Bacteriol.* **178,** 5263–5271
11. Severinov, K., Mustaev, A., Severinova, E., Bass, I., Kashlev., M., Landick, R., Nikiforov, V., Goldfarb, A., and Darst, S. A., (1995) *Proc. Natl. Acad. Sci. U. S. A.* **92,** 4591–4595
12. Severinov, K., Mustaev, A., Kukarin, A., Muzzin, O., Bass, I., Darst, S. A., and Goldfarb, A. (1996) *J. Biol. Chem.* **271,** 27969–27974
13. Kashlev, M., Martin, E., Polyakov, A., Severinov, K., Nikiforov, V., and Goldfarb, A. (1993) *Gene* **130,** 9–14
14. Severinov, K., Markov, D., Severinova, E., Nikiforov, V., Landick, R., Darst, S. A., and Goldfarb, A. (1995) *J. Biol. Chem.* **270,** 23926–23929
15. Gragerov, A. I., and Nikiforov, V. G. (1980) *FEBS Lett.* **122,** 17–20
16. Tang, H., Severinov, K., Goldfarb, A., and Ebright, R. H. (1995) *Proc. Natl. Acad. Sci. U. S. A.* **92,** 4902–4906
17. Borukhov, S., and Goldfarb, A. (1993) *Protein Expression Purif.* **4,** 503–511
18. Keana, J. F. W., and Cai, S. H. (1990) *J. Org. Chem.* **55,** 3640–3647
19. Nudler, E., Kashlev, M., Nikiforov, V., and Goldfarb, A. (1995) *Cell* **81,** 351–357
20. Laemmli, U. K. (1970) *Nature* **227,** 680–685
21. Orlova, M., Newlands, J., Das, A., Goldfarb, A., and Borukhov, S. (1995) *Proc. Natl. Acad. Sci. U. S. A.* **92,** 4596–4600
22. Honore, N., Bergh, S., Chanteau, S., Doucet-Populaire, F., Eiglmeier, K.,

Garnier, T., Georges, C., Launois, P., Limpaiboon, P., Newton, S., Nyang, K., del Potillo, P., Ramesh, G. K., Reddy, T., Riedel, J. P., Sittisombut, N., Wu-Nunter, S., and Cole, S. T. (1992) *Mol. Microbiol.* **7,** 207–214
23. Severinov, K., Mooney, R., Darst, S. A., and Landick, R. (1997) *J. Biol. Chem.* **272,** 24137–24140
24. Landick, R., Colwell, A., and Stewart, J. (1990) *J. Bacteriol.* **172,** 2844–2854
25. Weilbaecher, R., Hebron, C., Feng, G., and Landick, R. (1994) *Genes Dev.* **8,** 2913–2927
26. Krummel, B., and Chamberlin, M. J. (1992) *J. Mol. Biol.* **225,** 221–237
27. Nudler, E., Goldfarb, A., and Kashlev, M. (1994) *Science* **265,** 793–796
28. Komissarova, N., and Kashlev, M. (1997) *Proc. Natl. Acad. Sci. U. S. A.* **94,** 1755–1760
29. Komissarova, N., and Kashlev, M. (1997) *J. Biol. Chem.* **1272,** 15329–15338
30. Nudler, E., Mustaev, A., Lukhtanov, E., and Goldfarb, A. (1997) *Cell* **89,** 33–41
31. Archambault, J., Drebot, M. A., Stone, J. C., and Friesen, J. D. (1992) *Mol. Gen. Genet.* **232,** 408–414
32. Archambault, J., Lacroute, F., Ruet, A., and Friesen, J. D. (1992) *Mol. Cell. Biol.* **12,** 4142–4152
33. Wu, J., Awrey, D. E., Edwards, A. M., Archambault, J., and Friesen, J. D. (1996) *Proc. Natl. Acad. Sci. U. S. A.* **93,** 11552–11557
34. Luo, J., and Krakow, J. S. (1992) *J. Biol. Chem.* **267,** 18175–18181
35. Borukhov, S., Lee, J., and Goldfarb, A. (1991) *J. Biol. Chem.* **266,** 23932–23935
36. Koulich, D., Orlova, M., Malhotra, M., Sali, A., Darst, S. A., and Borukhov, S. (1997) *J. Biol. Chem.* **272,** 7201–7210
37. Ito, K., and Nakamura, Y. (1996) *Mol. Gen. Genet.* **251,** 699–706
38. Petersen, S. K., and Hansen, F. G. (1991) *J. Bacteriol.* **173,** 5200–5206
39. Stebbins, C. E., Borukhov, S., Orlova, M., Polyakov, A., Goldfarb, A., and Darst, S. A. (1995) *Nature* **373,** 636–640
40. Markovtsov, V., Mustaev, A., and Goldfarb, A. (1996) *Proc. Natl. Acad. Sci. U. S. A.* 93, 3221–3226
41. Landick, R., Stewart, J., and Lee, D. N. (1990) *Genes Dev.* **4,** 1623–1636
42. Mollet, C., Drancourt, M., and Raoult, D. (1998) *Gene* **207,** 97–104